DOI: 10.1002/chem.201002170

Sonoluminescence from OH($C^2\Sigma^+$) and OH($A^2\Sigma^+$) Radicals in Water: Evidence for Plasma Formation during Multibubble Cavitation

Rachel Pflieger,* Henri-Pierre Brau, and Sergey I. Nikitenko[a]

Nowadays spectroscopic studies of sonoluminescence (SL) have become a major tool to investigate the extreme conditions created by acoustic cavitation in liquids.[1] Soon after the discovery of SL, the importance of the nature of the dissolved gas was brought to light and it was shown that rare gases allowed brighter SL, with Xe leading to the highest SL intensity, followed by Kr and Ar .[2,3] However, whereas the influence of the rare-gas nature on the total light emission has been studied intensively, variations in the SL spectra have been subject to only a few investigations. In their SL spectra of water at 333 and 459 kHz in the presence of noble gases, Sehgal et al.[4] observed a broad continuum at 300–600 nm, attributed to $H + OH^{\bullet}$ recombination and possibly to the de-excitation of the water molecules or OH($B^2\Sigma^+$–$A^2\Sigma^+$) emission.[5] Sonoluminescence from OH($A^2\Sigma^+$–$X^2\Pi$) species (0–0 at ≈310 nm, 0–1 at ≈281 nm, 1–0 at ≈340 nm) was also observed under these conditions. Some years later, Gordeychuk et al.[6] published low-resolution SL spectra of water in the presence of Ar, Kr and Xe at a frequency of 863 kHz. They reported that the peak position of OH($A^2\Sigma^+$–$X^2\Pi$) emission at 310 nm did not depend on the dissolved gas, but that another maximum was present in the spectra: at 268 for Ar, 250 for Kr and 242 nm for Xe. These bands were attributed to the emission from excimers of water molecules with rare gases ($H_2O{\cdot}M$)*. More recently, Lepoint et al.[7] performed an analysis of the rovibronic structure of the OH($A^2\Sigma^+$–$X^2\Pi$) band at 20 kHz ultrasonic (US) frequency for water saturated with Ar and Kr. Their high-resolution SL spectra, though limited to the 300–350 nm range, clearly showed differences in the OH($A^2\Sigma^+$–$X^2\Pi$) features due to the saturating rare gas.

[a] Dr. R. Pflieger, H.-P. Brau, Dr. S. I. Nikitenko
Institut de Chimie Séparative de Marcoule (ICSM)
UMR 5257–CEA–CNRS–UMII–ENSCM, Centre de Marcoule
BP 17171, 30207 Bagnols sur Cèze Cedex, France
Fax: (+33) 466-79-76-11
E-mail: rachel.pflieger@cea.fr

Supporting information for this article is available on the WWW under http://dx.doi.org/10.1002/chem.201002170.

Concerning the influence of US frequency on the SL spectrum, only a few examples can be found in the literature. Didenko et al.[8] compared multibubble sonoluminescence (MBSL) spectra of Ar-saturated water at 22 kHz and at 863 kHz. They observed a more prominent OH band at 310 nm at 22 kHz, whereas at 863 kHz the 340 nm shoulder was more pronounced and the intensity in the UV region was higher (peaking at 270 nm). They explained these differences by the emission being not fully equilibrated. Beckett and Hua[9] measured Ar-saturated water spectra at 205, 358, 618 and 1071 kHz and obtained broad continuums that peaked around 300 nm. In general, the SL data reported in the literature for different US frequencies are hard to compare owing to very different experimental conditions (geometry of ultrasonic reactor, intensity of ultrasound, temperature, spectral resolution etc.). Herein, we report the study of multibubble SL at 200–450 nm in water in the presence of Ar, Kr and Xe at 20, 200 and 607 kHz US frequencies obtained under similar experimental conditions. For the first time we have observed SL from non-thermally excited OH($C^2\Sigma^+$) species.

The SL spectra were measured at each US frequency with the three rare gases Ar, Kr and Xe. All spectra present a continuum ranging from approximately 225 nm to the NIR; particular features are observed only in the 225–400 nm region, so only this region is shown in the presented spectra.

In all spectra OH($A^2\Sigma^+$–$X^2\Pi$) lines (≈270–350 nm) clearly stand out. The 0–0 and 1–1 lines are easy to distinguish, whereas the other two (1–0 and 0–1) are broad shoulders. These transitions are attributed according to recently published data.[7] Relative intensities of the vibrational electronic transitions depend upon the rare-gas nature and the US frequency. At 20 kHz (Figure 1) the main transition under Ar is 0–0 (310 nm), 1–0 (282-292 nm) is clearly defined, and a small 0–1 shoulder (≈337 nm) is visible. When Kr or Xe is used, the 1–0 transition almost disappears, the 0–1 transition gets more intense, and above all the 1–1 transition (≈315 nm) appears and becomes as intense as the 0–0 transition, and its intensity is even higher in Xe. At 200 kHz (Figure 2SI in the Supporting Information) the most inter-

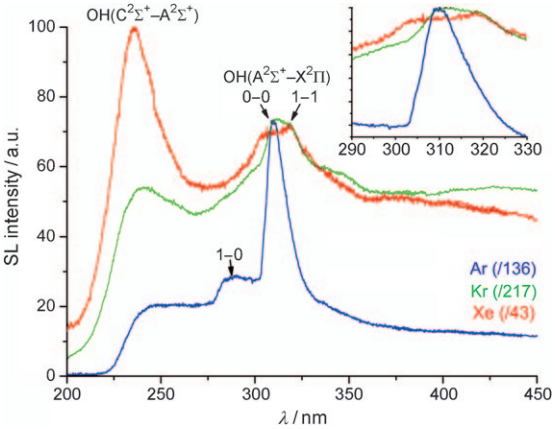

Figure 1. Effect of the rare gas on the 20 kHz SL spectra (10 °C, 0.09 W mL^{-1}; measurements were made close to the sonotrode for Ar and Kr, or 7 mm below the sonotrode for Xe, which explains why the measured intensity is lower in Xe). Insert: zoom around 310 nm.

esting feature is the variation of the population ratios between the 0–0 and 1–1 states when the gas is changed: in Ar $I_{0-0} > I_{1-1}$, in Kr $I_{0-0} \approx I_{1-1}$ and in Xe $I_{0-0} < I_{1-1}$. Also, the relative population of the 0–1 transition is higher in Kr and Xe, whereas that of 1–0 is lower in Xe. Similar variations in the vibrational transitions were observed at 607 kHz (Figure 2). In the presence of Ar (Figure 1 and Figure 3SI)

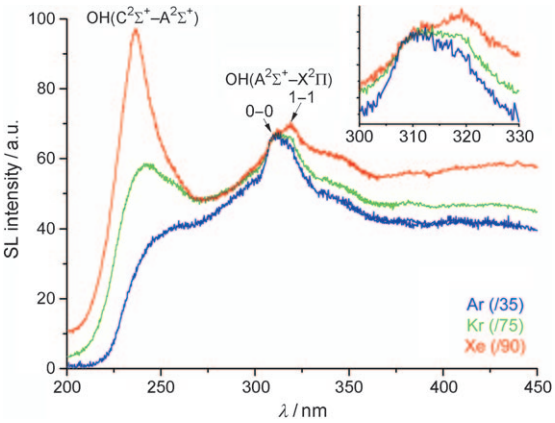

Figure 2. Effect of the rare gas on 607 kHz SL spectra (11 °C, 0.17 W mL^{-1}). Insert: zoom around 310 nm.

the 0–0 transition is very intense and is by far the major one at 20 kHz, whereas at higher frequencies there is a redistribution to the other vibrational transitions. In Xe (Figure 3), the 0–1 shoulder is more pronounced at high frequency and the 1–1 band is higher than the 0–0 one. According to the emission coefficients of 0–0 and 1–1,[10] under thermal equilibrium the intensity of 0–0 band should be higher than that of 1–1 band.[7] This is seen to be true only in Ar, whatever the US frequency. Thus, only the experimental SL spectra obtained with Ar can be fitted by using the program LIFBASE[11] (see the Supporting Information). A temperature

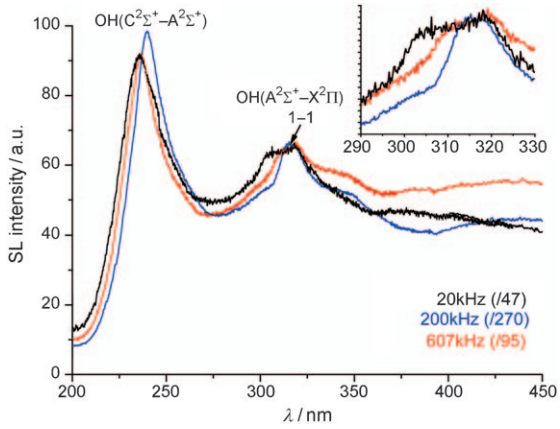

Figure 3. Effect of the US frequency on water/Xe SL spectra (10–11 °C, 0.17 W mL^{-1}). Insert: zoom around 310 nm.

of approximately 4000 K and pressure of 100–150 atm, usually considered as intrabubble conditions in the adiabatic heating model, are able to describe the OH($A^2\Sigma^+$–$X^2\Pi$) lines only in the case of Ar at 20 kHz. At 200 and 607 kHz under Ar, the simulation gives temperatures of, respectively, approximately 9000 and 7000 K and pressures of, respectively, approximately 250 and 220 atm. The relatively strong intensity I_{1-1} indicates deviation from thermal equilibrium in Kr and Xe and higher population of more excited vibrational states. This behaviour is more pronounced at high frequency (especially at 200 kHz). In particular, in Xe at 200 kHz, the 0–0 band is apparently not present. This feature could not be observed in previous studies,[4,6,8,12] in which the resolution was not sufficient.

The most interesting change induced by the rare gases in the SL spectra is, however, not in the OH($A^2\Sigma^+$–$X^2\Pi$) transition band but in the appearance and development of another band around 230–250 nm. At 20 and at 607 kHz, this band is discernable in Kr (Figures 1 and 2). At 200 kHz it is well visible in Ar, and the curve in Kr is similar (Figure 2SI in the Supporting Information). In Xe it is the main band whatever the US frequency (Figure 3). In addition, the maximum of this band, which is not very discernable in Ar, is slightly shifted between Kr and Xe, and also when the frequency is changed as shown in Table 1.

We attribute this band to the OH($C^2\Sigma^+$–$A^2\Sigma^+$) electronic transition.[5] This band is actually never observed in flames[13] but it is seen in electrical discharges through water vapour[14–16] and in water radiolysis.[17,18] One of the six vibra-

Table 1. Wavelengths [nm] of the maximum emission in the OH($C^2\Sigma^+$–$A^2\Sigma^+$) vibrational electronic transitions. Because the signals are large, their maximum wavelength is only given as an approximate value.

US frequency [kHz]	Gas		
	Ar	Kr	Xe
20	–	241	236
200	237	244	240
607	–	242	237

tional bands computed by Mohan[5] is particularly populated here: 1–7 (246.5 nm). Also, two bands calculated by Wallace[19] are observed here: 0–6 (237.0 nm) and 1–8 (240.6 nm). The 240.6 nm transition may correspond to the emission observed by Nath and Khare[20] in their laser-induced breakdown experiments in water. The most probable mechanism of the OH($C^2\Sigma^+$) state production involves[18] excitation of the water molecule by collision with a sufficiently energetic electron. The excited H_2O molecule must possess an excitation energy of at least 16.1 eV to form OH($C^2\Sigma^+$) excited species. The existence of OH$^\bullet$ species with different electronic temperatures also indicates deviation from thermal equilibrium during cavitation bubble collapse. This is in line with the recently reported Treanor effect during carbon monoxide sonochemical disproportionation in water.[21] Therefore, the present data clearly point to non-thermal plasma formation during multibubble cavitation in water in the presence of Kr and Xe. This indication of more extreme conditions is consistent with higher SL yields observed when these gases are used. Until now, formation of non-thermal plasma was reported only in concentrated H_2SO_4 in the presence of rare gases.[22–24] Another clue for temperature inhomogeneity during MBSL was reported in sulfuric acid,[25] though without evidence for plasma formation.

In conclusion, this work underlines the dramatic effect of the gas nature and of the ultrasonic frequency on the SL spectra of water, and in particular on the relative populations of the OH$^\bullet$ radical excited states. Moreover, OH($C^2\Sigma^+$–$A^2\Sigma^+$) emission gives clear evidence for plasma formation during multibubble cavitation in water. This finding highlights that MBSL, and consequently multibubble sonochemistry, cannot be interpreted only as an adiabatic or quasi-adiabatic thermal process. It supports the idea[26] that MBSL light emission is (at least) partly due to emission from plasma and furthermore gives evidence that the latter plasma is non-thermal.

Experimental Section

The multifrequency ultrasonic device is shown in the Supporting Information together with the experimental details. The thermostated cylindrical reactor was mounted on top of the high-frequency transducer (200 or 607 kHz, L3 communications ELAC Nautik). Ultrasonic irradiation with low-frequency ultrasound of 20 kHz was performed with a titanium horn (Vibra-Cell) placed reproducibly on top of the reactor. Deionised water (250 mL) was continuously sparged with the desired saturating gas (Ar, Kr, Xe; 99.999 %; Air Liquide). The cryostat temperature was set to have a steady-state temperature of 10–11 °C within the sonoreactor. Spectra were recorded by using a spectrometer (SP 2356i; Roper Scientific) coupled to a liquid-nitrogen cooled CCD camera (SPEC10–100BR with a UV coating; Roper Scientific). Each spectrum was the average of at least three 120 s spectra (sometimes 60 s for Kr and Xe) that were corrected for background noise and for the quantum efficiencies of the gratings and CCD.

Acknowledgements

The authors wish to thank Laurent Couston (CEA/DEN/Marcoule) for useful discussions.

Keywords: frequency · luminescence · radicals · sonoluminescence · ultrasound

[1] K. S. Suslick, D. J. Flannigan, *Ann. Rev. Phys. Chem.* **2008**, *59*, 659–683.
[2] R. O. Prudhomme, *Bulleid Meml. Lect. Bull. Soc. Chim. Biol.* **1957**, 39, 425–430.
[3] F. R. Young, *J. Acoust. Soc. Am.* **1976**, *60*, 100–104.
[4] C. Sehgal, R. G. Sutherland, R. E. Verrall, *J. Phys. Chem.* **1980**, *84*, 388–395.
[5] H. Mohan, Shardanand, *US NTIS* **1975**, NASA-SP-373.
[6] T. V. Gordeychuk, Y. T. Didenko, S. P. Pugach, *Acoust. Phys.* **1996**, *42*, 240–241.
[7] T. Lepoint, F. Lepoint-Mullie, N. Voglet, S. Labouret, C. Petrier, R. Avni, J. Luque, *Ultrason. Sonochem.* **2003**, *10*, 167–174.
[8] Y. T. Didenko, T. V. Gordeychuk, *Phys. Rev. Lett.* **2000**, *84*, 5640–5643.
[9] M. A. Beckett, I. Hua, *J. Phys. Chem. A* **2001**, *105*, 3796–3802.
[10] J. Luque, D. R. Crosley, *J. Chem. Phys.* **1998**, *109*, 439–448.
[11] J. Luque, D. R. Crosley, SRI International Report MP 99-009, **1999**.
[12] Y. T. Didenko, S. P. Pugach, *J. Phys. Chem.* **1994**, *98*, 9742–9749.
[13] G. Zizak, lecture given at the ICS Training Course on Laser Diagnostics of Combustion Processes, NILES, University of Cairo (Egypt), **2000**.
[14] A. K. Shuaibov, A. A. Heneral, Y. O. Shpenik, Y. V. Zhmenyak, I. V. Shevera, R. V. Gritsak, *Tech. Phys.* **2009**, *54*, 1238–1240.
[15] A. Michel, *Z. Naturforsch. A* **1957**, *12*, 887–896.
[16] C. Carlone, F. W. Dalby, *Can. J. Phys.* **1969**, *47*, 1945–1957.
[17] D. N. Sitharamarao, J. F. Duncan, *J. Phys. Chem.* **1963**, *67*, 2126–2132.
[18] T. I. Quickenden, J. A. Irvin, D. F. Sangster, *J. Chem. Phys.* **1978**, *69*, 4395–4402.
[19] L. Wallace, *Astrophys. J. Suppl. Ser.* **1962**, *7*, 165–290.
[20] A. Nath, A. Khare, *J. Phys. Conf. Ser.* **2010**, *208*, 012090.
[21] S. T. Nikitenko, P. Martinez, T. Chave, I. Billy, *Angew. Chem.* **2009**, *121*, 9693–9696; *Angew. Chem. Int. Ed.* **2009**, *48*, 9529–9532.
[22] N. C. Eddingsaas, K. S. Suslick, *J. Am. Chem. Soc.* **2007**, *129*, 3838–3839.
[23] D. J. Flannigan, K. S. Suslick, *Nature* **2005**, *434*, 52–55.
[24] D. J. Flannigan, K. S. Suslick, *Phys. Rev. Lett.* **2005**, *95*, 044301.
[25] H. X. Xu, N. G. Glumac, K. S. Suslick, *Angew. Chem.* **2010**, *122*, 1097–1100; *Angew. Chem. Int. Ed.* **2010**, *49*, 1079–1082.
[26] K. Yasui, T. Tuziuti, M. Sivakumar, Y. Iida, *Appl. Spectrosc. Rev.* **2004**, *39*, 399–436.

Received: July 29, 2010
Published online: September 6, 2010

